Three-Dimensional Structure of the Oligosaccharide Chain of GM1 Ganglioside Revealed by a Distance-Mapping Procedure: A Rotating and Laboratory Frame Nuclear Overhauser Enhancement Investigation of Native Glycolipid in Dimethyl Sulfoxide and in Water–Dodecylphosphocholine Solutions

Domenico Acquotti,[†] Leszek Poppe,[‡,§] Janusz Dabrowski,*[,‡] Claus-Wilhelm von der Lieth,[∥] Sandro Sonnino,[†] and Guido Tettamanti[†]

Contribution from the Study Center for Functional Biochemistry of Brain Lipids, Department of Medical Chemistry and Biochemistry, The Medical School, University of Milan, Via Saldini 50, 20133 Milano, Italy, Max-Planck-Institut für Medizinische Forschung, Jahnstrasse 29, D-6900 Heidelberg, Germany, and Deutsches Krebsforschungszentrum, D-6900 Heidelberg, Germany. *Received October 16, 1989*

Abstract: Three-dimensional structure of the oligosaccharide part of the GM1 ganglioside, Galβ1-3GalNAcβ1-(NeuAcα2-3)4Galβ1-4Glcβ1-1Cer, was modeled with use of a distance-mapping procedure that was based on NOE contacts between amido, hydroxy, and C-linked protons, observed for the intact ganglioside dissolved in Me_2SO-d_6. The glycosidic linkages of the branched core trisaccharide segment are significantly more rigid than the linkages of the external disaccharide Galβ1-3GalNAc and Galβ1-4Glc segments, which exist in several conformations. The conformation of the sialic acid side chain seems to be predominantly determined by the hydrogen bond between the C(8)–OH proton and either the carboxylic or ring oxygen, whereas the presence of the acetyl substituent of the C(5)–amino group is irrelevant for this conformation. Similar conformations were found for GM1 anchored in mixed D_2O/dodecylphosphocholine-d_{38} micelles.

Gangliosides, amphiphilic molecules characterized by the presence of sialic acid residue(s), are components of the plasma membrane of vertebrate cells, being particularly abundant in the nervous system.[1] They are asymmetrically located in the outer face of the membrane with the oligosaccharide portions that protrude from the cell surface interacting with a variety of external ligands.[2] The interaction between ganglioside GM1 [Galβ1-3GalNAcβ1-4(NeuAcα2-3)Galβ1-4Glcβ1-1Cer] and *Cholerae toxin*, for example, has been studied in great detail,[3] and the derived information led to the hypothesis that gangliosides are directly involved in the processes of specific recognition of signal molecules at the membrane surface and signal transduction through the membrane.[4]

The specific interaction with external ligands and the generation of accompanying effects implies both a fit chemical structure of the ganglioside and a matching three-dimensional (3D) shape (conformation) of its molecules. The conformation of *N*-acetylneuraminic acids and gangliosides has been investigated experimentally by NMR[5] and theoretically with the hard sphere exoanomeric (HSEA) approach[6] or semiempirical potential functions.[7] Since the results of these investigations were partly at variance with one another, it is important further to investigate ganglioside conformations by taking advantage of new methodological and computational developments in this field.

In this study we investigated the conformation of native GM1, i.e., with its hydroxy and amido protons unexchanged for deuterium. NMR signals of hydroxy and amido protons can readily be observed in Me_2SO solution and are a useful additional source of interatomic contact information.[8] It is vital to this approach that NOE and proton-exchange cross-peaks can be discriminated by their opposite phase in rotating frame NOE spectra (ROESY), as this feature eliminates possible misinterpretations. Moreover, the virtual absence of spin diffusion in ROESY experiments excludes de facto another source of false contact information. On the other hand, some contact information might get lost, since weak NOEs may be cancelled by the three-spin effect. Notwithstanding this minor limitation, several times more NOE contacts of diagnostic value can be obtained by this method than was possible with deuterium-exchanged samples. The avaibility of several NOE contacts for each sugar residue opens the possiblity to define glycosidic bond conformations entirely in geometrical terms. In this paper we rationalize NOE data by mapping the NOE-derived interatomic distances in Φ,Ψ coordinates referring to the two glycosidic bond angles.

Since the acetamido group of the *N*-acetylneuraminic acid is believed to participate in a set of hydrogen bonds[5a,b] and thus can be supposed to affect the conformation of gangliosides, we investigated the corresponding deAcetyl GM1 ganglioside (deAc-GM1) under the same conditions for comparison.

Gangliosides form in water nonspherical micelles of large molecular weight and hydrodynamic radius,[9a] their mobility being reduced so severely as to prevent obtaining high-resolution NMR spectra. However, the natural cell-surface environment of

* Author to whom correspondence should be addressed.
† University of Milan.
‡ Max-Planck-Institut für Medizinische Forschung.
§ Present address: Complex Carbohydrate Research Center, The University of Georgia, Athens, GA 30602.
∥ Deutsches Krebsforschungszentrum.

(1) Wiegandt, H. *Adv. Neurochem.* **1982**, *4*, 149–223.
(2) (a) Heiningen van, W. E. *Nature* **1974**, *249*, 415–417. (b) Brady, R. O.; Fishman, P. H. *Adv. Enzymol. Relat. Areas Mol. Biol.* **1979**, *50*, 303–323.
(3) (a) Fishman, P. H. *J. Membr. Biol.* **1982**, *69*, 85–97. (b) Fishman, P. H. *Chem. Phys. Lipids* **1986**, *42*, 137–151.
(4) Fishman, P. H. In *New Trends in Ganglioside Research*; Ledeen, R. W., Hogan, E. L., Tettamanti, G., Yates A. J., Yu, R. K., Eds.; Liviana Press: Padova, Italy, 1988.
(5) (a) Brown, E. B.; Brey, S. W.; Weltner, W. *Biochim. Biophys. Acta* **1975**, *399*, 124–130. (b) Czarniecki, M. F.; Thornton, E. R. *J. Am. Chem. Soc.* **1977**, *99*, 8273–8279. (c) Sillerud, L. O.; Yu, R. K.; Schafer, D. E. *Biochemistry* **1982**, *21*, 1260–1271. (d) Koerner, T. A. W.; Prestegard, J. H.; Demou, P. C.; Yu, R. K. *Ibid.* **1983**, *22*, 2676–2687. (e) Christian, R.; Schulz, G.; Brandstetter, H. H.; Zbiral, E. *Carbohydr. Res.* **1987**, *162*, 1–11. (f) Breg, J.; Kroon-Batenburg, L. M. J.; Strecker, G.; Montreuil, J.; Vliegenthart J. F. G. *Eur. J. Biochem.* **1989**, *178*, 727–739. (g) Poppe, L.; Dabrowski, J.; Lieth, C.-W., v. d.; Numata, M.; Ogawa, T. *Ibid.* **1989**, *180*, 337–342.
(6) (a) Sabesan, S.; Bock, K.; Lemieux, R. U. *Can. J. Chem.* **1984**, *62*, 1034–1045. (b) Bock, K. In *Gangliosides and Neuronal Plasticity*; Tettamanti, G., Ledeen, R. W., Sandhoff, K., Nagai, Y., Toffano, G., Eds.; Liviana Press: Padova, Italy, 1986.
(7) (a) Veluraja, K.; Rao, V. S. R. *Carbohydr. Polym.* **1983**, *3*, 175–192. (b) Veluraja, K.; Rao, V. S. R. *Biochim. Biophys. Acta* **1980**, *630*, 442–446.
(8) Dabrowski, J.; Poppe, L. *J. Am. Chem. Soc.* **1989**, *111*, 1510–1511.
(9) (a) Corti, M.; Degiorgio, V.; Sonnino, S.; Ghidoni, R.; Masserini, M.; Tettamanti, G. *Chem. Phys. Lipids* **1981**, *28*, 197–214. (b) Tettamanti, G.; Bonali, F.; Marchesini, S.; Zambotti, V. *Biochim. Biophys. Acta* **1973**, *296*, 160–170.

0002-7863/90/1512-7772$02.50/0

Table I. Chemical Shifts[a] for Oligosaccharide Protons of GM1 and deAc-GM1 (Italicized) in Me_2SO-d_6 at 297 K

residue		1	2	3	4	5	6	6′	7	8	9R	9S	Ac
Glcβ	CH	4.14	3.03	3.32	3.27	3.39	3.63	3.73					
		4.15	*3.03*	*3.31*	*3.32*	*3.27*	*3.64*	*3.71*					
	OH		5.13	4.55			4.59						
			5.14	*4.58*			*4.60*						
Galβ	CH	4.26	3.13	3.70	3.94	3.47	3.47	3.64					
		4.19	*3.12*	*3.71*	*3.92*	*3.51*	*3.41*	*3.63*					
	OH		5.03				4.30						
			5.12				*4.31*						
NeuAcα	CH			2.53 eq	3.71	3.34	3.05		3.16	3.47	3.34	3.63	1.87
				1.67 ax									
Neuα				*2.54* eq	*3.69*	*2.70*	*3.38*		*3.45*	*3.51*	*3.40*	*3.70*	
				1.65 ax									
NeuAcα	OH				4.72	(8.03)[b]			4.71	5.97	4.89		
Neuα					5.30				*4.64*	*6.06*	*5.03*		
GalNAcβ	CH	4.89	3.91	3.43	3.69	3.64	3.45	3.47					1.73
		4.86	*3.91*	*3.43*	*3.71*	*3.63*	*3.45*	*3.47*					*1.77*
	OH		(7.68)[b]		4.34		4.58						
			(*7.57*)[b]		*4.33*		*4.56*						
Galβ	CH	4.18	3.32	3.28	3.59	3.36	3.49	3.53					
		4.18	*3.28*	*3.34*	*3.60*	*3.32*	*3.51*	*3.53*					
	OH		3.68	4.78	4.40		4.86						
			3.73	*4.80*	*4.42*		*4.91*						

[a] Chemical shifts in ppm are relative to dimethyl sulfoxide set equal to 2.49 ppm. [b] NH.

gangliosides in the physiological medium of water can be approached by investigating them in the form of mixed micelles obtained with the aid of perdeuterated detergents[10] such as sodium dodecylsulfate or dodecylphosphocholine. Micelles of this type, if obtained with a low concentration of ganglioside, are smaller compared to the aggregates of pure ganglioside and show a much higher rotational mobility, thus allowing high-resolution NMR spectra to be recorded. Here, we compare the conformations of GM1 and deAc-GM1 determined in Me_2SO and in mixed micelles, respectively.

Materials and Methods

GM1 ganglioside was extracted from calf brain according to the process given by Tettamanti et al.,[9b] purified, and transformed into sodium salt,[9a] which was used for all measurements. DeAc-GM1 was prepared and purified as already described.[11] Deuterated solvents (Me_2SO-d_6 and D_2O) and dodecylphosphocholine-d_{38} (DPC) were purchased from Merck, Sharp & Dohme.

^{1}H NMR Spectroscopy. GM1 and deAc-GM1 (4 mg), previously lyophilized and dried under high vacuum, were dissolved in Me_2SO-d_6 (0.4 mL). Mixed micelles were prepared by dissolving gangliosides and the detergent (molar ratio 1:40) in deuterated 50 mM phospate buffer (0.5 mL); the mixture was exchanged three times with D_2O, with intermediate lyophilization, dried under high vacuum, and finally dissolved in D_2O.[10] Spectra were obtained at a frequency of 500 MHz with use of a Bruker AM 500 spectrometer equipped with an Aspect 3000 computer, a process controller, an array processor, and a selective excitation unit. Chemical shifts were referenced to Me_4Si either directly (for micelles) or indirectly (for other solutions) by setting the ^{1}H signal of residual Me_2SO-d_5 at 2.49 ppm. One-dimensional homonuclear Hartman–Hahn spectroscopy (1D HOHAHA) experiments were performed by selective excitation with a DANTE pulse sequence, followed by a MLEV-17 sequence for spin-lock[12] and a z-filter[12,13] for the purging phase or multiplet distorsions. The mixing time was varied from 50 to 160 ms to obtain various degrees of magnetization transfer. Spectral assignments were obtained from two-dimensional (2D) HOHAHA experiments; in particular the 2D HOHAHA experiment for the DPC–water solution of deAc-GM1 was run in the TPPI mode with the MLEV-17 pulse sequence for spin-lock[14] with a saturation DANTE pulse for the residual water signal. The mixing time was 170 ms and the spectral width was 3 kHz. Transient 1D ROESY and NOESY experiments were performed with direct subtraction of reference FIDs every eight scans, with a total accumulation of 800 transients per spectrum. For selective irradiation a shaped pulse or DANTE pulse were used. Two-dimensional (2D) ROESY spectra were measured by the pulse sequence devised by Rance.[15] The spin-lock was placed between two 170° pulses whose amplitudes were twice the locking rf power (2.6 kHz) to improve the magnetization transfer efficiency.[16] Baseline distorsions were minimized by applying a Hahn–echo sequence immediately before the aquisition[17] and adjusting the receiver phase to the pure absorbtion mode.[18] The rf carrier was placed about 1–1.5 kHz downfield, relative to the center of proton resonances during the spin-lock time, and at the center during evolution and aquisition. The spectra were recorded at 297–303 K with 400–800 t_1 increments and 64 scans were collected for each t_1. Mixing time was in the range 80–160 ms. Spectral width was 4–5 kHz. After zero filling the time domain spectra were transformed to give a $4K \times 2K$ real points matrix with the resolution of 3.91 and 1.95 Hz/point in the ω_1 and ω_2 dimension, respectively. For band-selective 2D ROESY experiments with ω_1 decoupling the pulse sequence was a variant developed from that mentioned above[15] by combining frequency band-selective and nonselective pulses[19] in order to minimize overlap of cross-peaks. Measurements were run with irradiating selectively at 4.4 ppm with 90° and 180° Gaussian pulses of 8 ms truncated at the 2% level and a mixing time of 154 ms; 128 transients for each t_1 experiment were collected. The spectral width was 4000 Hz in ω_2 and 400 Hz in ω_1 and the spectral size in the time domain was 4096 × 128. Prior to Fourier transformation, the time domain data were zero filled to 8192 × 512. NOESY spectra (2D) were measured in the TPPI mode by using the pulse sequence by Bodenhausen et al.,[20] with a selective DANTE pulse during the relaxation delay to saturate the residual water signal. Spectra, recorded at 308 K with 512 t_1 increments (64 scans for each) and a spectral width of 4000 Hz, were zero-filled to give a $2K \times 1K$ matrix with a resolution of 5.8 and 2.9 Hz/point in ω_1 and ω_2 dimensions, respectively. All 2D spectra were weighted with the squared sine bell function shifted by $(\pi/2)$ in both dimensions.

Distance-Mapping Procedure. The "NOE distances" r_{kl} for the proton pair H_k–H_l were obtained from the equation $r_{kl} = r_{ij}(V_{ij}/V_{kl})^{1/6}$, where V_{kl} and V_{ij} are the cross-peak volumes for unknown and calibration distances, respectively, measured by the standard Bruker 2D integration routine from 2D ROESY and 2D NOESY spectra. The exchange contribution to cross-peak volumes for hydroxyl protons was insignificant. The distance mapping procedure was performed on an IBM 3090 computer as described in the preceding article.[21] The populations for different rotational states of pendent groups were estimated on the basis of

(10) Eaton, H.; Hakomori S. I. Third Chemical Congress of North America, Toronto, 1988; Abstract No. CARB 91.
(11) Sonnino, S.; Kirshner, G.; Ghidoni, G.; Acquotti, D.; Tettamanti, G. *J. Lipid Res.* **1985**, *26*, 248–257.
(12) Subramanian, S.; Bax, A. *J. Magn. Reson.* **1987**, *71*, 325–330.
(13) Sorensen, O. W.; Rance, M.; Ernst, R. R. *J. Magn. Reson.* **1984**, *56*, 527–534.
(14) Bax, A.; Davis, D. G. *J. Magn. Reson.* **1985**, *65*, 355–360.
(15) Rance, M. *J. Magn. Reson.* **1987**, *74*, 557–564.
(16) Dezheng, Z.; Fujiwara, T.; Nagayama, K. *J. Magn. Reson.* **1989**, *81*, 628–630.
(17) Davis, D. G. *J. Magn. Reson.* **1989**, *81*, 603–607.
(18) Marion, D.; Bax, A. *J. Magn. Reson.* **1988**, *79*, 352–356.
(19) Brüschweiler, R.; Griesinger, C.; Sorensen, O. W.; Ernst, R. R. *J. Magn. Reson.* **1988**, *78*, 178–185.
(20) Bodenhausen, G.; Kogler, H.; Ernst R. R. *J. Magn. Reson.* **1984**, *58*, 370–388.
(21) Poppe, L.; Lieth, C.-W. v.d.; Dabrowski, J. *J. Am. Chem. Soc.* Preceding paper in this issue.

Table II. Coupling Constants (Hz) and Temperature Coefficients κ (-10^{-3} ppm/deg C) for Amido and Hydroxy Protons of GM1 and deAc-GM1 (Italicized) in Me_2SO-d_6

residue		J	κ	residue		J	κ
Glcβ (I)	OH2	3.7	5.19	GalNAcβ (III)	OH4	4.9	7.42
		3.6	*5.66*			*4.6*	*7.60*
	OH3	<2	2.84		OH6	5.2	4.38
		<2	*2.60*			*4.9*	*4.85*
	OH6	5.8	5.39		NH2	8.2[a]	2.88
		5.6	*6.58*			*9.2*	*0.82*
Galβ (II)	OH2	5.2	7.51	Galβ (IV)	OH2	<2	<1
		5.2	*7.76*			<2	*1.15*
	OH6	6.4	3.37		OH3	5.2	7.56
		5.6	*3.42*			*5.2*	*8.83*
NeuAcα (N)	OH4	5.2	4.49		OH4	5.2	5.62
		4.7[a]	*3.08*			*4.4*	*6.43*
	OH7	3.7	3.27		OH6	6.1	3.11
		8.2	*6.12*			*5.9*	*4.64*
	OH8	3.0[a]	<1				
		3.0[a]	*1.54*				
	OH9	6.1	10.67				
		5.9	*12.20*				
	NH5	8.5	4.80				

[a] Broad signal.

NOE contacts with the ring protons and vicinal coupling constants by using Karplus type equations developed for hydroxyl,[22] amido,[23] and hydroxymethylene[24] groups. The sterically allowed areas were calculated for the minimum possible atom–atom approach.[21] For all computations the coordinates for sugar ring atoms were taken from the Cambridge Crystallographic Data Bank.

The MM2 calculations were run on the same computer with use of Allingers MM2(85) program;[25] the dielectric constant input was 1.5.

Results and Discussion

Spectral assignments of GM1 and deAc–GM1, together with vicinal coupling constants and temperature coefficients for hydroxy and amido protons, are given in Tables I and II.

Conformational analysis of the pentasaccharide moiety of GM1 ganglioside is based predominantly on geometrical considerations, and the reliability of experimentally derived structures was further substantiated by MM2 calculations.

The basis source of structural information is interresidual NOE contacts, obtained from 2D ROESY spectra (Figure 1) and listed in Table III and mapped in the Φ,Ψ space of each glycosidis linkage through the procedure described in the preceding paper.[21]

The Conformation of the Branched Trisaccharide Fragment, GalNAcβ1-(NeuAcα2-3)4Gal. The 3D structure of this moiety was of special interest, since possible through-space interactions between the directly not bonded glycosidic substituents at the vicinal sites Gal–O3 and –O4 could be expected to affect the relative orientation of all three of these residues. In particular, the potentially adaptable NeuAc glycerol side chain was likely to play a role in this respect, hence it was rational first to analyze its conformation.

The H6–C6–C7–H7 (θ_1) and H7–C7–C8–H8 (θ_2) dihedral angles can be derived from vicinal coupling constants $^3J_{6,7}$ and $^3J_{7,8}$, respectively. Although the Karplus equation[24] gives two alternative solutions for each ^3J value, the correct one can be chosen by "NOE labeling", i.e., by locating the vicinal protons relative to some other protons firmly localized in the molecule (the intraresidual NOE contacts for the glycerol side chain and both amido groups are gathered separately in Table IV). In this way, dihedral angles $\theta_1 = -60°$ and $\theta_2 = -160°$ were obtained, and a number of further observations suggest that the side chain is fairly rigid in this geometry. Thus, the vanishingly small $^3J_{H8,OH8}$ coupling constant (<2 Hz vs ~6 Hz for a freely rotating OH group; cf. Table II), the small temperature shift of the OH8

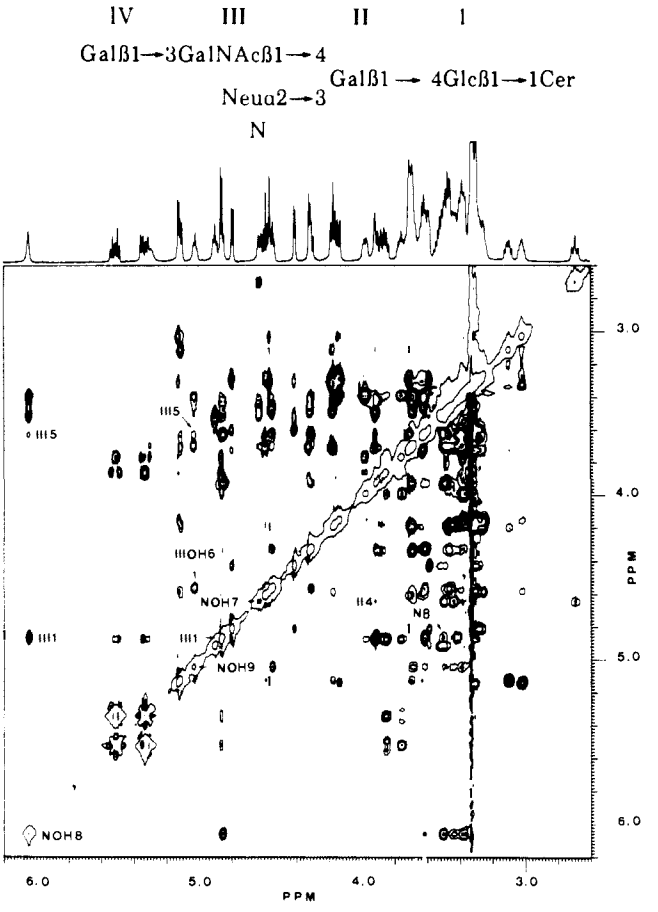

Figure 1. Partial 2D 500-MHz ^1H NMR ROESY spectrum of deAc-GM1 (mixing time 200 ms; offset during spin-lock time, 6.51 ppm) in Me_2SO-d_6 at 297 K with some of the interresidual contacts indicated (for other NOE contacts, see Figures 2, 5, 6, 8, and 10).

resonance (Table II), and a strong OH8/H6 NOE contact (Table IV) point to a hydrogen bond between the OH8 proton and either the carboxylic NO1 oxygen or the NO6 ring oxygen. The former of these two hydrogen bonds seems to be more probable in view of the exceptionally large low-field shift of the NOH8 proton, as compared with the chemical shift of the IOH3 proton that is hydrogen bonded to the IIO5 ring oxygen (6 ppm vs 4.5 ppm; vide infra); MM2 calculations also favor the formation of this type of hydrogen bond (vide infra). On the other hand a hydrogen bond to the ring oxygen would form a thermodynamically more stable pseudo-five-membered ring, hence this problem is worthy of further investigation. The situation did not change after the removal of the *N*-acetyl group of sialic acid. Indeed, the vicinal coupling constants $J_{6,7}$ and $J_{7,8}$ remained unchanged for deAc-GM1, and also the OH8 signal showed the same behavior. Furthermore, it appeared that in GM1 the OH7 proton is hydrogen bonded with the carbonyl oxygen of the *N*-acetyl group, since it showed a significantly smaller coupling constant and chemical shift temperature coefficient (Table II), and a smaller NOE distance to the H5 proton (2.3 vs 2.9 Å), than in the case of deAc-GM1. An additional argument for the existence of this hydrogen bond is the favorable conformation of the acetamido group characterized by a torsional angle H–N–C5–H5 close to 150°, as determined from the vicinal coupling constant and NOE contacts (Table IV and Figure 2). Although some ambiguity concerning the intramolecular hydrogen bonding remains, the suggested conformation of the *N*-acetylneuraminic acid side chain (Figure 3) differs substantially from the structures proposed in earlier studies by Brown et al.[5a] and Czarniecki and Thornton.[5b] On the other hand, the same conformation was proposed by Sabesan et al.,[6a] Christian et al.,[5e] and Poppe et al.,[5g] but no conclusions concerning intraresidual hydrogen bonds were drawn.

The vicinal coupling constants for the prochiral methylene protons, H9*R* and H9*S*, have significantly different values and

(22) Fraser, R. R.; Kaufman, M.; Morand, P. *Can. J. Chem.* **1968**, *47*, 403–409.
(23) Bystrov, V. F.; Portnova, S. L.; Balashova, T. A.; Kozmin, S. A.; Gavrilov, Y. D.; Afanasev, V. A. *Tetrahedron* **1973**, *29*, 873–877.
(24) Haasnoot, C. A. G.; de Leeuw, F. A. A. M.; Altona, C. *Tetrahedron* **1980**, *36*, 2783–2792.
(25) Burkert, U.; Allinger, N. L. *Molecular Mechanics*; American Chemical Society: Washington, DC, 1982; ACS Monogr. 177.

Table III. Interresidual Contacts for GM1 and deAc-GM1 Molecules and the Corresponding NOE Distances, r^*_{kl}

residue	contacts	r^*_{kl}, Å	contacts	r^*_{kl}, Å	contacts	r^*_{kl}, Å
Galβ	IV-1/III-2	3.5	IV-1/III-NH	3.5		
	IV-1/III-3	2.5	IV-OH2/III-Ac	3.9		
	IV-1/III-4	3.5				
	IV1/III-Ac	3.8[a]				
GalNAcβ	III-1/II-4	2.2	III-1/N-OH8	2.6	III-OH6/II-OH6	3.1
	III-1/N-8	3.1	III-5/N-OH8	3.5	III-OH6/N-OH9	2.4
	III-Ac/II-2	3.1	III-5/N-OH9	3.3		
			III-Ac/II-OH2	3.7[a]		
			III-OH6/N-9*R*	3.6		
			III-NH/II-2	3.6		
Galβ	II-1/I-4	2.4	II-OH2/I-6	3.6	II-OH2/I-OH3	3.5
	II-1/I-6′	3.1	II-OH2/I-6′	3.4	II-OH2/I-OH6	>4
			II-1/I-OH3	3.3		
			II-6/I-OH3	3.5		
			II-1/I-OH6	>4		
NeuAcα (N)	N-3ax/II-3	2.1	N-3ax/II-OH2	3.2		
			N-3eq/II-OH2	2.9		
			N-OH7/II-4	3.3		

[a] The distance to the methyl carbon was calibrated from the NH–Ac interaction.

Table IV. Intraresidual Contacts and Corresponding NOE Distances, r^*_{kl}, for the NH Protons of the NeuAc and GalNAc Residues and the Side-Chain Protons of the NeuAc Residue

residue	contacts	r^*_{kl}, Å	residue	contacts	r^*_{kl}, Å
NeuAcα	N-7/N-5	3.1	GalNAcβ	III-NH/III-1	2.6
(N)	N-7/N-6	2.7	(III)	III-NH/III-2	2.9
	N-7/N-8	2.9		III-NH/III-3	2.7
	N-7/N-9*S*	3.6			
	N-7/N-9*R*	3.0			
	N-OH7/N-5	2.3			
	N-OH8/N-6	2.4			
	N-NH/N-4	2.4			
	N-NH/N-5	2.8			
	N-NH/N-6	2.8			
	N-NH/N-7	3.2			
	N-NH/N-OH4	2.6			

can be readily assigned by NOE labeling[5g] with respect to H7 (Table IV). Assuming that a hydroxymethyl group can occupy three staggered conformations, the population ratio for *gg*, *gt*, and *tg* conformers, obtained with the aid of a modified Karplus equation,[24] is equal to 0.5:0.5:0.

The conformation of the sialic acid side chain remains almost the same for GM1 and deAc-GM1 anchored in DPC micelles in aqueous solution, as inferred from coupling constant patterns (Table VI) and also from NOE interaction with the GalNAc residue (vide infra).

The NOE distance map for the NeuAc2-3Gal linkage in GM1 is depicted in Figure 4. Is shows a well-defined conformation with glycosidic angles Φ,Ψ close to −165° and −18°, respectively. It is interesting to note that the same linkage in GM4 (NeuAcα2-3Galβ1-1Ceramide) showed conformational averaging among three sterically allowed regions in Me_2SO and between two confomations in D_2O solutions[5g] and that averaging was also observed for the NeuAcα2-3Galβ1-4GlcNAcβ1-NAsn glycopeptide.[5f] This different conformational behaviour of GM1 is readily explainable by the vicinal location of the GalNAc residue, which is probably hydrogen bonded to the sialic acid side chain (vide infra) and locks the NeuAcα2-3Gal linkage in one conformation. For micelle-bound GM1 (and deAc-GM1) the situation should be similar, as evidenced by the same distance, 2.1

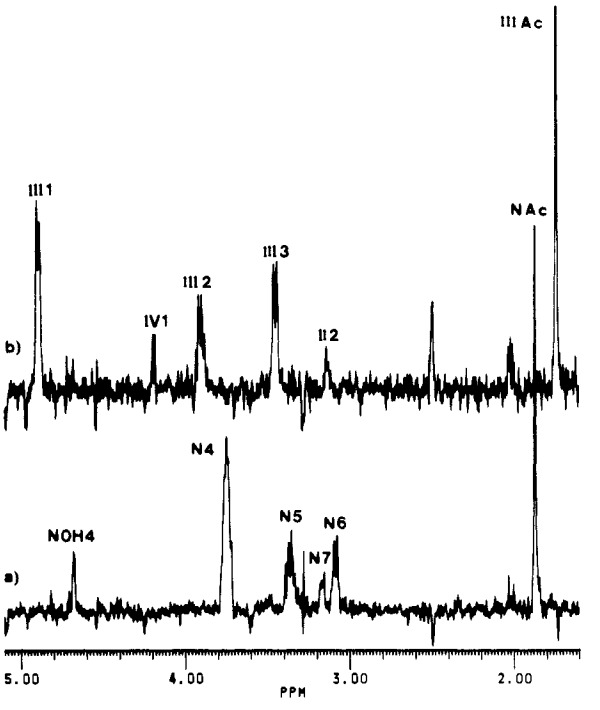

Figure 2. Cross sections from the 2D ROESY spectrum through the sugar NH proton resonances. For labeling, see the formula in Figure 1.

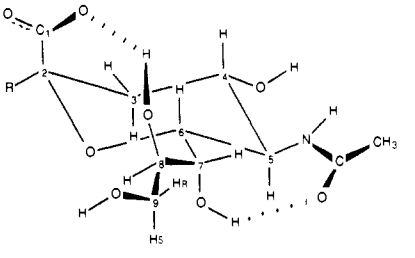

Figure 3. Proposed conformation of the *N*-acetylneuraminic acid residue in GM1 ganglioside, based on NOE and vicinal coupling constants.

Table V. Chemical Shifts (ppm) of Oligosaccharide Protons for deAc-GM1[a] in DPC/D_2O Solution at 308 K

residue	1	2	3	4	5	6	6′	7	8	9*R*	9*S*	Ac
Glcβ (I)	4.49	3.38		[3.60–3.68][b]		3.83[c]	4.02[c]					
Galβ (II)	4.55	3.39	4.16	4.15	3.77[c]	3.63[c]	3.80[c]					
GalNAcβ (III)	4.81	4.08	3.85	4.20	3.76[c]	3.83[c]	3.83[c]					
Galβ (IV)	4.58	3.57	3.68	3.96	3.73[c]	3.78[c]	3.78[c]					2.04
Neuα (N)			1.97 ax	3.82	3.10	3.66		3.84	3.80	3.73	3.92	
			2.72 eq									

[a] Chemical shifts for GM1 were practically identical with those obtained by Eaton and Hakomori.[10] [b] The H3, H4, and H5 protons of the glucose ring are strongly coupled and have overlapped chemical shifts in the range 3.60–3.68 ppm. [c] Assigned by NOE and relayed NOE.

Table VI. Vicinal Coupling Constants (Hz) for the GM1 *N*-Acetylneuraminic Acid Side Chain in Me_2SO-d_6 and DPC/D_2O Solutions[a]

^3J	6,7	7,8	8,9*S*	8,9*R*
DPC/D_2O	<2	8.5	2.4	5.9
Me_2SO	<2	8.7	2.1	6.5

[a] The same values, within experimental error, were found for deAc-GM1.

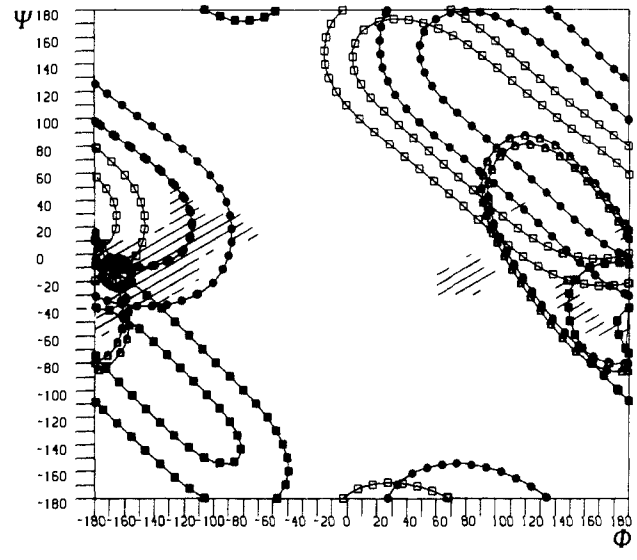

Figure 4. NOE map for the NeuAcα2-3Galβ linkage. NOE-derived constraints are marked with the following symbols: (●) NH3ax/IIOH2; (□) NH3eq/IIOH2; (■) NOH7/IIH4; (Δ) NH3ax/IIH3.

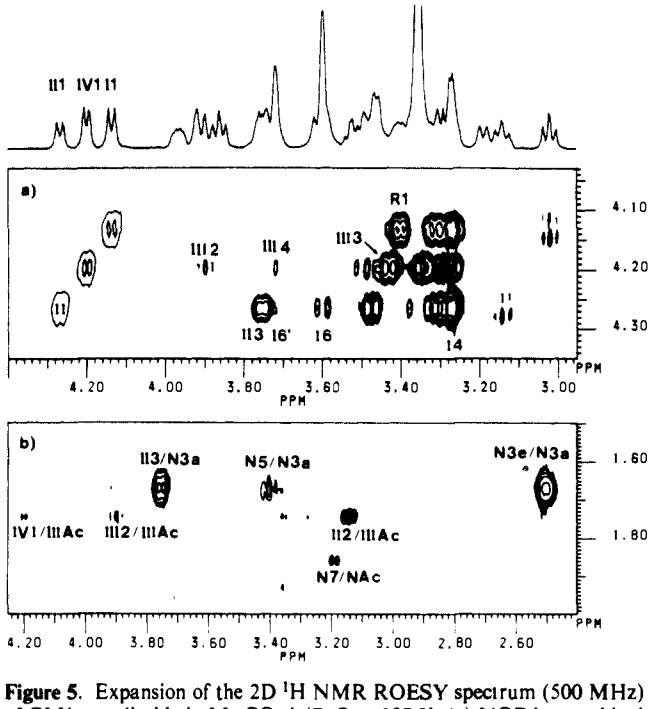

Figure 5. Expansion of the 2D ^1H NMR ROESY spectrum (500 MHz) of GM1 ganglioside in Me_2SO-d_6/D_2O at 307 K: (a) NOE interresidual contacts for anomeric protons of Glcβ (I), Galβ (II), and Galβ (IV), (b) NOE contacts for the acetyl groups of NeuAcα (N) and GalNAcβ (III) residues.

Å, between the NH3ax and IIH3 protons, as well as by the IIIH1–NH8 interaction (Figures 5b and 6a).

The conformation of the GalNAcβ1-4Galβ linkage was first analyzed by mapping distance constraints obtained from NOE contacts between these two units (Figure 7). For the amido proton, dipolar interactions both to the protons of its parent ring (Table IV and Figure 2) and to the protons of the neighboring

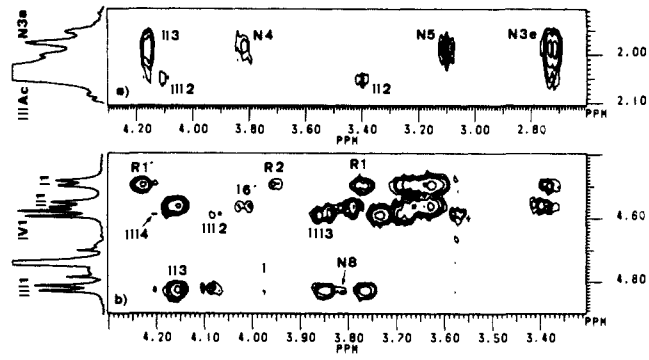

Figure 6. Expansion of the 2D ^1H NMR NOESY spectrum (500 MHz) of a deuterated DPC–water solution of deAc-GM1 at 308 K (mixing time, 200 ms): (a) NOE contacts with NH3ax and IIIAc and (b) with anomeric protons. The corresponding parts of the 1D spectra are shown on the left side of the contour plot.

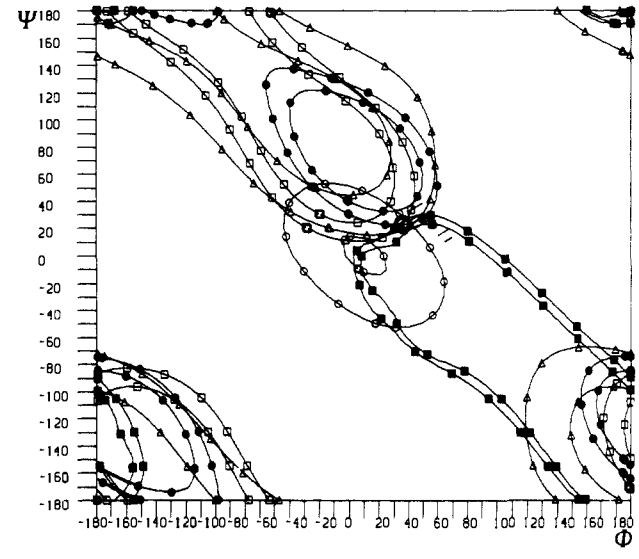

Figure 7. NOE map for the GalNAcβ1-4Galβ linkage. NOE-derived constraints are marked with the following symbols: (●) IIIH1/IIH4; (○) IIIAc/IIH2; (□) IIIAc/IIHO2; (■) IIIOH6/IIOH6; (Δ) IIINH/IIH2.

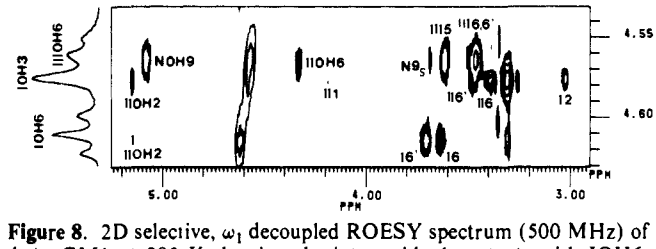

Figure 8. 2D selective, ω_1 decoupled ROESY spectrum (500 MHz) of deAc-GM1 at 293 K showing the interresidual contacts with IOH6, IOH3, and NOH9; the coupled 1D spectrum of these hydroxy groups is shown on the left. The IIH1/IOH3 contact appears weak at this temperature because the competing indirect IOH3/IH3/IIH1 ROE magnetization transfer signal has an opposite phase and diminishes the observed peak volume.

residues (Table III and Figure 2), as well as the large vicinal coupling constant (9.5 Hz), strongly suggest that the acetamido group exercises torsions, of approximately ±30°, around the value 180° for dihedral angle defined by H–N–C–H atoms. Consequently, for calculating distance constraints involving amido and methyl protons (Figure 7a) the acetamido group was held for simplification in the 180° position.

At all temperatures suitable for NOE measurements, the IIIOH6 and IOH3 signals were overlapped and it was necessary to perform a 2D selective and ω_1 decoupled ROESY experiment[19] to prove the existence of the IIIOH6/IIOH6 NOE interaction (Figure 8). For the mapping procedure of this constraint both these exocyclic groups were assumed to be uniformly populated,

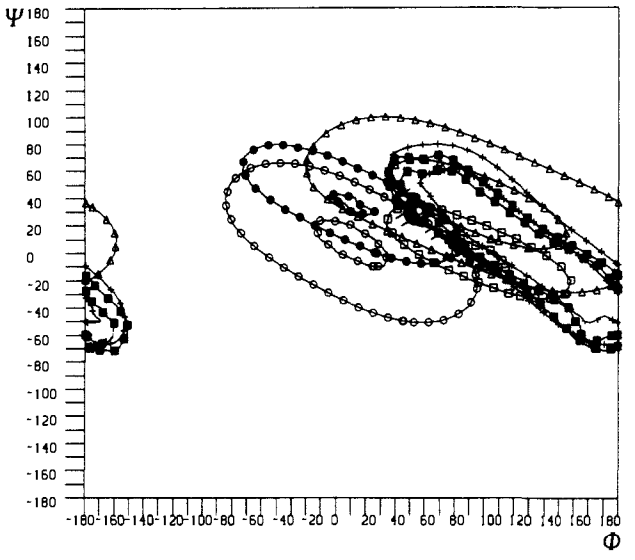

Figure 9. NOE-derived constraints between NeuAc and GalNAc units plotted in Φ,Ψ space of GalNAcβ1-4Galβ linkage. The Φ,Ψ and θ_1,θ_2 angles for NeuAcα2-3Galβ and C8–C7–C6 linkages were −165°, −18° and −60°, −160°, respectively. Labeling of the constraints: (○) IIIH1/NH8; (●) IIIH1/NOH8; (□) IIIH5/NOH9; (■) IIIOH6/NOH9; (△) IIIH5/NOH8; (+) IIIOH6/NH9*R*.

since the vicinal coupling constants for methylene protons were close to 6 Hz. The primary hydroxyl and IIOH2 protons were found to populate uniformly all staggered rotational states, as estimated on the basis of vicinal coupling constants ($^3J_{CH_2,OH}$ and $^3J_{H,OH}$) and NOE contacts to the ring protons (II2, II1, II3).

The plot in Figure 7 clearly shows that glycosidic angles of the GalNAcβ1-4Galβ linkage sample the Φ,Ψ space in the vicinity of 30°,25°. The conformation of this linkage was modeled independently by analysis of NOE contacts between the GalNAc residue and the sialic acid side chain (Figure 9). For the distance mapping procedure, the conformation of the NeuAcα2-3Gal linkage and the sialic acid side chain, except for its terminal CH_2OH group, was held constant. The OH8 group was kept in the g^- (∠H–O–C–H = −60°) conformation, a uniform distribution was assumed for the OH9 proton, and the populations for the methylene group were input as given earlier (vide supra). We generated several NOE maps for slightly different conformations (up to ±20° for each torsional angle) of the NeuAcα2-3Gal and C8–C7–C6 linkages and found the area of maximum overlap close to 50°,30° in Φ,Ψ space of the GalNAcβ1-4Galβ linkage. These values belong to the sterically allowed area (hatched in Figure 9) and do not differ much from those found in Figure 7 (30°,25°), thus pointing to a restricted freedom for both of the glycosidic angles Φ and Ψ. It is highly probable that hydrogen bonds involving the hydroxy group pairs IIOH6/IIIOH6 and IIIOH6/NOH9 may form and break during the conformational transitions of all these exocyclic groups. The conformations in this area are also favorable for a hydrogen bond between the NH group of the GalNAc residue and the carboxylic group of sialic acid. The proximity of these two groups is clearly supported by the dramatic high-field shift, from 7.60 to 6.58 ppm, occurring upon addition of trifluoroacetic acid to a solution of sodium carboxylate of GM1 in Me_2SO, while the other two amide protons (from NeuAc and ceramide) remain practically unaffected.[26] Unfortunately, the behavior of hydroxyl protons cannot be followed during the pH changes because of their fast exchange rate.

A similar conformation for the GalNAcβ1-4Galβ linkage was found in the aquous solution of deAc-GM1 anchored in the DPC micelle. The $IIICH_3$/IIH2 NOE contact is clearly visible in 2D NOESY spectra (Figure 6a). We have also proved the existence of the important IIIH1/NH8 interaction evidencing spatial

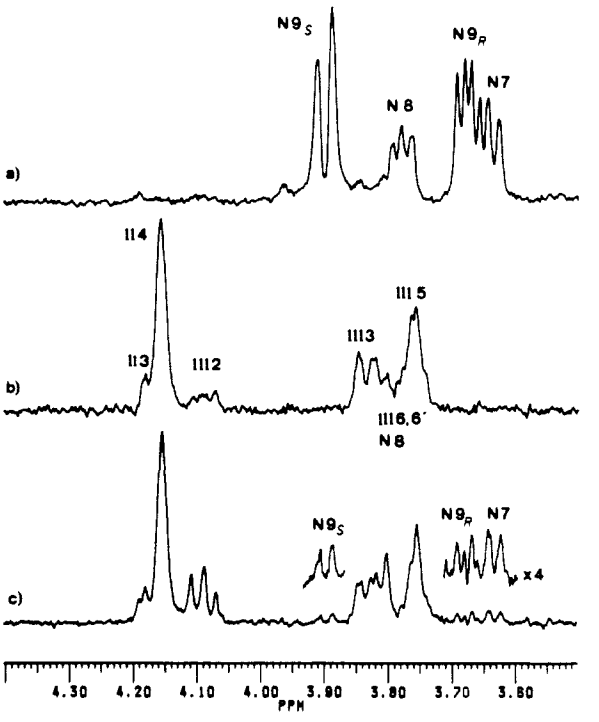

Figure 10. 500-MHz 1D spectra of a deuterated DPC–water solution of GM1 ganglioside at 325 K: (a) HOHAHA spectrum obtained by selective irradiation of the NH9*S* proton, (b) ROESY spectrum obtained by selective inversion of the IIIH1 magnetization, with rf carrier set at 4.7 ppm during the spin-lock time, (c) as in (b), but with rf carrier set at 3.73 ppm during the spin-lock time. Mixing time and effective lock field in (b) and (c) were 200 ms and 2.3 kHz.

proximity between two not directly bonded residues, which needs some comment, however. Because of a prohibitively strong overlap of several resonances in the relevant spectral region of deAc-GM1 (Table V), we took advantage of a slightly more favorable distribution of the GM1 resonances and assumed that the conformations of the two compounds are alike, similarly as was the case in Me_2SO solution. It was still not possible to directly establish this interaction, since the overlap of the NH8 with the IIIH6,6′ resonances around 3.8 ppm and the small spectral interval between the latter and the IIIH5 resonance ($\Delta\delta \approx 35$ Hz) opens two alternative ways for the selectively excited IIIH1 proton to produce a response in the 3.8-ppm region: (i) by IIIH1/NH8 cross relaxation, or (ii) by IIIH1/IIIH5 cross relaxation with subsequent IIIH5/III H6,6′ magnetization transfer via spin diffusion or the Hartmann–Hahn mechanism. In order to circumvent this difficulty, we carried out the experiments presented in Figure 10, which provided information equivalent to that obtainable from a relayed ROE (ROTO[27]) experiment. The NH7,8,9*R*,9*S* signals were first unambiguously identified by using a HOHAHA scheme (Figure 10a). The 1D ROE difference spectrum (Figure 10b) obtained by a selective inversion of the IIIH1 magnetization, with the spin-locking rf carrier offset by ca. 1 ppm from the NH8 resonance, produced a number of intra- and interresidue NOE signals, but the presence of the NH8 signal was uncertain because of the ambiguity just discussed. If, however, the carrier was placed close to the NH8 chemical shift (Figure 10c), the NH7,9*R*,9S responses became clearly visible, which can only be explained by a ROE-type magnetization transfer from IIIH1 to NH8 followed by Hartmann–Hahn transfer from NH8 to NH7,9R,9S.

For modeling the 3D structure of the core trisaccharide fragment under discussion, we performed MM2 calculations, starting from structures derived experimentally, i.e. dihedral bond angles were input as obtained from maximum overlap of NOE constraints (for glycosidic bonds this is shown in Figures 4, 7, and 9; the analogous diagram for the sialic acid side chain is not shown).

(26) Fronza, G.; Sonnino, S.; Acquotti, D.; Ghidoni, R. Proceedings of the 8th International Symposium on Glycoconjugates, Houston, 1985; p 472.

(27) Kessler, H.; Gemmecker, G.; Haase, B. *J. Magn. Reson.* **1988**, *77*, 401–408.

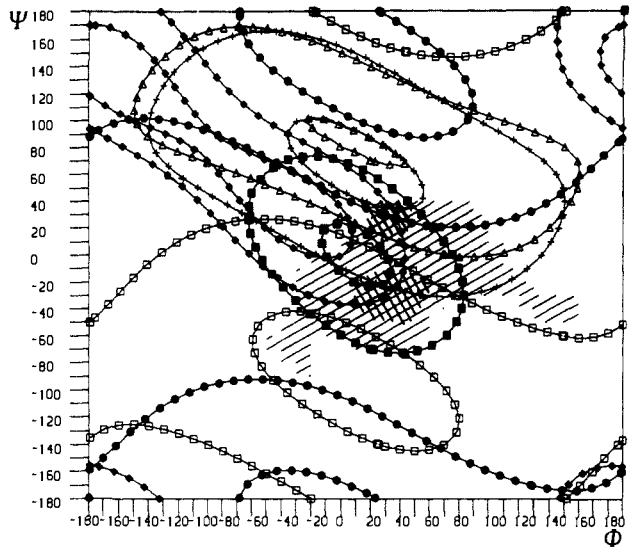

Figure 11. NOE map for Galβ1-3GalNAc linkage. NOE-derived constraints are marked with the following symbols: (●) IVH1/IIIH2; (□) IVH1/IIIH4; (■) IVH1/IIIH3; (Δ) IVH1/IIIAc; (+) IVH1/IIINH; ((⊠) IVOH2/IIIAc.

The hydroxy, methylene, and acetamino pendent groups were input in the conformations favoring hydrogen bond formations discussed before. We also restarted the calculations from different sets of dihedral angles, mostly varying the initial conformation of the sialic acid side chain. The results clearly showed the lowest energy minima for structures characterised by the Φ,Ψ dihedral angles III–II = 50 ± 10°, 18 ± 3°, = N–II = −168 ± 5°, −16 ± 3°, and θ_2, θ_1 dihedral angles falling within the ranges −155 ± 5°, −55 ± 5°, respectively. The carboxylic group was twisted, the NO1–C1–C2–NO6 angle being close to −40° and thus favoring the hydrogen bond formation involving the NO1 and NO8 oxygens. Indeed, in all low-energy structures the separation between these atoms was close to 2.9 Å, whereas the NO6–NO8 distance was greater then 3.1 Å, which is the upper limit for hydrogen bond formation.

The Conformation of the Galβ1-3GalNAcβ and Galβ1-4Glcβ Linkages. The NOE representation of the terminal Galβ1-3GalNAcβ linkage is shown in Figure 11. The two areas of overlap (grated) around (Φ,Ψ) values of (25°,30°) and (30°,−40°) demonstrate a pronounced flexibility of glycosidic angle Ψ, similar to that found for GalNAcβ1-3Galα linkage in globoside.[21] The IVH1/IIIH2 and IVH1/IIIH4 NOE cross peaks, which can only arise when the angle Ψ changes its value by ca. 70°, are shown in Figure 5a for GM1 in DMSO and in Figure 6b for aqueous solution. In the latter solution these contacts were also confirmed by a 1D ROESY experiment performed with selective inversion of the IVH1 magnetization (not shown).

The NOE contacts for the Galβ1-4Glcβ linkage appear in Table III and are the same as those found for the same linkage in globoside; as was shown in the preceding paper,[21] this linkage occupies at least four different conformations with glycosidic angles Φ,Ψ close to 55°,0°; 35°,−50°; 5°,−30°, and 30°,−170° (or 170°,−5°), the appearence of the last two conformers being evidenced by the IIOH2/IOH3 NOE contact (Figure 8). The behavior of the IOH3 resonance (Table II) is characteristic of IOH3···IIO5 hydrogen bonding, similarly as in the previous studies of glycosphingolipids.[5g,21] In micelle-bound GM1, only the IIH1/IH4 and IIH1/IH6 contacts could be observed (Figure 6b), which are characteristic of the (55°,0°) conformer. Nevertheless, this linkage probably experiences the same flexibility in aqueous solution, similarly as found for cellobiose in theoretical and experimental studies summarized recently by Stevens and Santhyanarayana.[28]

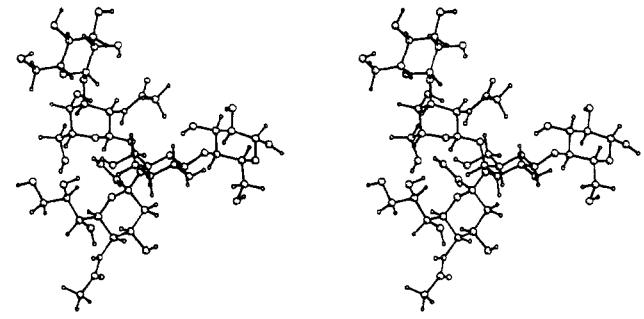

Figure 12. Stereoplot of the low-energy conformation of GM1 oligosaccharide obtained from distance mapping followed by MM2 energy minimization.

The MM2 calculations for the whole pentasaccharide were started from the previously optimized conformation of the core trisaccharide. The II–I linkage was input in the 50°,0° conformation, and about 20 structures with differing conformation for the IV–III linkage were generated. It seems reasonable to assume that conformational changes of IV–III and II–I linkages are not correlated, hence it was not necessary to repeat the calculations from different starting conformations of the II–I linkage. The final structures confirmed the experimentally documented variability of angle Ψ of the IV–III linkage, in that Φ,Ψ angles for this linkage were close to 30°,30° and 20°,−40° in the low-energy conformations.

In Figure 12 is shown the stereodiagram of GM1 pentasaccharide in one of its minimum energy conformations characterized by the following set of angles: IV–III − 33.9°, 31.6°; III–II = 41.5°, 20.1°; θ_1 = −57.3°; θ_2 = −156.7°; N–II = −170.0°, −19.9°; II–I = 51.4°, −7.4°.

The conformation of the branched trisaccharide segment found in this work is in good agreement with the structures proposed on the basis of NMR and hard-sphere calculations by Sabesan et al.[6] and potential energy calculations by Veluraja and Rao.[7] These authors predicted, however, one preferred conformation for each of the outer disaccharide segments, Galβ1-3GalNAc and Galβ1-4Glc, whereas flexibility for both of these linkages was clearly shown in this study.

Acknowledgment. D.A. was supported by a fellowship from the Fondazione Anna Villa Rusconi and L.P. from the Max-Planck-Gesellschaft. This work was also supported by a grant to J.D. from the Fritz Thyssen Stiftung.

Registry No. GM1 ganglioside, 37758-47-7.

Supplementary Material Available: Listing of cross-peak volumes obtained from 2D ROESY spectra recorded for solutions in Me_2SO-d_6 at different temperatures and for different mixing times (3 pages). Ordering information is given on any current masthead page.

(28) Stevens, E. S.; Sathyanarayana, B. K. *J. Am. Chem. Soc.* **1989**, *111*, 4149–4154.